

# An Efficient and Ecofriendly $\text{WO}_x\text{-ZrO}_2$ Solid Acid Catalyst for Classical Mannich Reaction

Benjaram M. Reddy · Meghshyam K. Patil ·  
Baddam T. Reddy

Received: 28 March 2008 / Accepted: 5 May 2008 / Published online: 28 May 2008  
© Springer Science+Business Media, LLC 2008

**Abstract** An ecofriendly  $\text{WO}_x\text{-ZrO}_2$  solid acid catalyst has been employed for the synthesis of  $\beta$ -amino ketones by a three-component Mannich reaction in the liquid phase under solvent-free conditions at ambient temperature. To make the  $\text{WO}_x\text{-ZrO}_2$  catalyst,  $\text{WO}_x$  from ammonium metatungstate was incorporated into the hydrous zirconia and calcined at 923 K. The incorporated promoter showed a strong influence on the surface and bulk properties of the zirconia. Surface and bulk properties of the catalyst were investigated by means of X-ray powder diffraction, temperature programmed desorption of ammonia, Raman spectroscopy, scanning electron microscopy, and BET surface area methods. Characterization studies reveal that the  $\text{WO}_x\text{-ZrO}_2$  catalyst exhibits strong solid acidity. The catalytic activity results suggest that the methodology adopted offers significant improvements for the synthesis of  $\beta$ -amino ketones with regard to yield of products, simplicity in the operation, and green aspects by avoiding toxic conventional catalysts and solvents.

**Keywords** Solid acid ·  $\text{WO}_x\text{-ZrO}_2$  · Mannich reaction ·  $\beta$ -Amino ketones · Amines · Catalyst characterization

## 1 Introduction

Acid catalysts play a predominant role in organic synthesis and transformation reactions. Many organic reactions, such as alkylation, acylation, isomerization, nitration, esterification, and rearrangements like pinacol, Beckman, etc., are

accomplished by acid catalysts. All these acid catalyzed reactions are mostly carried out by employing conventional mineral acids like  $\text{H}_2\text{SO}_4$ ,  $\text{HNO}_3$ , and HF or Lewis acids, such as  $\text{AlCl}_3$  and  $\text{BF}_3$ . In view of environmental and economical reasons, there is an ongoing effort to replace the conventional catalysts with newer solid acids. This is mainly due to some distinct advantages of certain solid acid catalysts, such as non-toxicity, non-corrosiveness, ease of handling, less expensive, and easy to recover and reuse [1–6]. Accordingly, various solid acid catalysts, such as heteropolyacids, ion exchange resins (Amberlyst and Nafion-H), zeolites, and clays were investigated [7–9]. The main disadvantage associated with heteropolyacids is that they are fairly soluble in polar solvents and lose their activity at higher temperatures by losing structural integrity. To prevent this, there are some attempts to immobilize them in silica or activated carbon matrix, which however limits the accessibility and efficiency of the catalytic active phase. Ion exchange resins exhibit poor thermal stability and low specific surface area. Styrene-based resins like Amberlyst is stable up to 393–413 K but its acid strength and surface area are not very high ( $H_0 = -2.2$ ,  $SA = 0.4 \text{ m}^2 \text{ g}^{-1}$ ). Nafion-H exhibits better thermal stability (533–553 K) and acidity than Amberlyst but possesses less specific surface area ( $H_0 = -12$  to  $-13$ ,  $SA = 0.02 \text{ m}^2 \text{ g}^{-1}$ ) [5]. Although clays and zeolites are quite reliable, activities of these materials are much lower than the conventional homogeneous acids due to pore blocking and hydration. In view of these reasons, there is an ongoing effort to develop stronger solid acids which are water tolerant, stable at high temperatures and suitable for both liquid and vapor phase conditions. On those lines, metal oxide-based catalysts offer several advantages over zeolites and clay-based catalysts. The metal oxide-based catalysts are active over a wide range of temperatures and more resistant to thermal excursions.

B. M. Reddy (✉) · M. K. Patil · B. T. Reddy  
Inorganic and Physical Chemistry Division, Indian Institute of  
Chemical Technology, Uppal Road, Hyderabad 500 607, India  
e-mail: mreddyb@yahoo.com

Among various solid acid catalysts that were reported, sulfated zirconia (SZ) gained much attention due to its high activity and efficiency to catalyze many reactions even at low temperatures [10–16]. However, the SZ catalyst gets deactivated rapidly at high temperatures and in reducing atmosphere by forming  $\text{SO}_x$  and  $\text{H}_2\text{S}$ , respectively. Also it forms sulfuric acid if there is water in the reaction medium leading to down-stream contamination. Arata and Hino reported that the solid superacids could be synthesized by incorporating  $\text{WO}_x$  or  $\text{MO}_x$  into Zr- or Ti-hydroxides under certain preparation conditions [17, 18]. Thus, tungstated zirconia (TZ) catalyst received some attention and was explored for various reactions. Interestingly, the TZ catalyst exhibited good catalytic activity for various organic synthesis and transformation reactions, such as acetylation of alcohols, phenols, and amines [19], alkylation of phenols [20], and synthesis of coumarins [21].

The use of ecofriendly solid acid catalysts for organic synthesis and transformation reactions in the liquid phase under solvent-free or with environmentally benign solvents represent an ideal green chemical technology protocol from both environmental and economical point of view. To the best of our knowledge, this will be one of the promising approaches for the synthesis of  $\beta$ -amino ketones by a three-component Mannich-type reaction in the liquid phase under solvent-free conditions at ambient temperature employing a simple and inexpensive TZ solid acid catalyst. The Mannich reaction is a classical method for the preparation of  $\beta$ -amino ketones and aldehydes [22–24], and has been one of the most important basic reactions in organic chemistry for its use in natural product and pharmaceutical syntheses. The present study deals with the synthesis of TZ catalyst and its characterization by various physicochemical techniques namely, X-ray diffraction, BET surface area, temperature programmed desorption (TPD) of ammonia, Raman spectroscopy, and scanning electron microscopy. The prepared catalyst was evaluated for the title reaction in the liquid phase under solvent-free conditions at ambient temperature.

## 2 Experimental Section

### 2.1 Catalyst Preparation

Zirconium hydroxide was prepared from zirconium oxy-chloride by hydrolysis with dilute aqueous ammonia solution. For this purpose, the requisite quantity of  $\text{ZrOCl}_2 \cdot 8\text{H}_2\text{O}$  (Loba Chime, GR grade) was dissolved in doubly distilled water and to this clear solution, aqueous  $\text{NH}_3$  was added drop-wise with vigorous stirring until the pH of the solution reached 8. The obtained precipitate was washed with hot distilled water several times until free

from chloride ions and dried at 393 K for 24 h. On the obtained  $\text{Zr}(\text{OH})_4$ , a nominal 10 wt.%  $\text{WO}_x$  was deposited by adopting a wet impregnation method. To achieve this, the requisite quantity of ammonium metatungstate (BDH Chemical Ltd, AR grade) was dissolved in doubly distilled water and to this clear solution the desired quantity of oven dried  $\text{Zr}(\text{OH})_4$  was added and the excess water was evaporated on a water-bath. The resulting cake was oven dried at 393 K for 24 h and calcined at 923 K for 6 h in a flow of oxygen. A small portion of the hydrous zirconia was calcined at 923 K for 6 h to make unpromoted  $\text{ZrO}_2$ .

### 2.2 Catalyst Characterization

The powder X-ray diffraction patterns were recorded on a Siemens D-5000 diffractometer by using  $\text{Cu K}\alpha$  radiation source and scintillation counter detector. The X-ray crystalline phases were identified by comparison with the reference data from PDF-ICDD files. The BET surface areas were obtained by  $\text{N}_2$  physisorption at liquid  $\text{N}_2$  temperature on a Micromeritics Gemini 2360 instrument. Before measurements, samples were oven dried at 393 K for 12 h and flushed with Argon gas for 2 h. Raman spectra were recorded at ambient temperature on a DILOR XY spectrometer equipped with a CCD detector. The spectra were recorded in the range of  $4,000\text{--}100\text{ cm}^{-1}$  and at a spectral resolution of  $2\text{ cm}^{-1}$  using the 514.5 nm excitation line from an argon ion laser (Spectra Physics, USA). The temperature programmed desorption measurements were carried on an Auto Chem 2910 instrument (Micromeritics, USA). A thermal conductivity detector was used for continuous monitoring of the desorbed ammonia and the areas under the peaks were integrated using GRAMS/32 software. Prior to TPD studies, samples were pretreated at 473 K for 1 h in a flow of ultra pure helium gas ( $40\text{ mL min}^{-1}$ ). After pretreatment, the sample was saturated with 10% ultra pure anhydrous ammonia gas (balance He,  $75\text{ mL min}^{-1}$ ) at 353 K for 2 h and subsequently flushed with He ( $60\text{ mL min}^{-1}$ ) at 373 K for 2 h to remove the physisorbed ammonia. The heating rate for the TPD measurements, from ambient to 1,023 K, was  $10\text{ K min}^{-1}$ . The SEM analyses were carried out with a Hitachi model-520 instrument. The finely powdered samples were mounted on a silver sample holder with the help of an adhesive to make the sample surface conductive and were coated with gold metal at 10 mm Hg pressure.

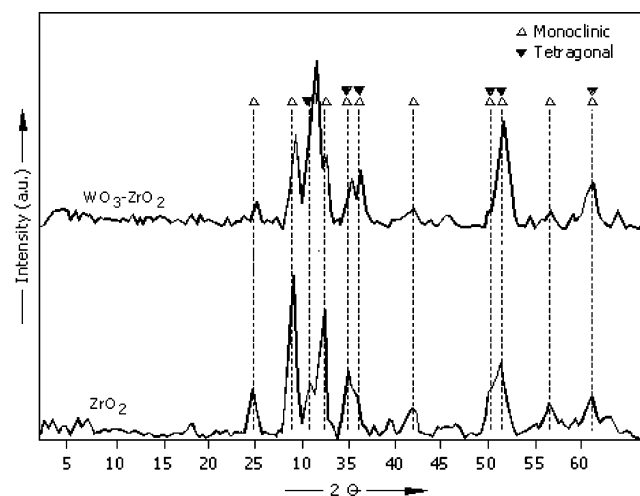
### 2.3 Activity Studies

All chemicals used in this study were commercially available and used without further purification. In a typical reaction procedure, an aromatic aldehyde, aromatic amine and ketone in 1:1:4 mole ratio, respectively, were taken in

a batch reactor and a 50 mg of catalyst was added. The reaction mixture was stirred in nitrogen atmosphere under solvent-free conditions at ambient temperature. Completion of the reaction was monitored by TLC. After completion of the reaction, catalyst was recovered by simple filtration, and reused. The products were recovered from the filtrate, concentrated on a rotatory evaporator and chromatographed on a silica gel column to afford pure products (isolated yields). NMR, IR, and mass spectroscopic techniques were used to analyze the products and compared with the authentic samples.

### 3 Results and Discussion

The X-ray powder diffraction patterns of tungstate ion promoted zirconia sample along with unpromoted ZrO<sub>2</sub> are shown in Fig. 1. The corresponding phase composition and crystallite size measurements are presented in Table 1. As shown in Fig. 1, the unpromoted zirconia is in a poorly crystalline form with monoclinic ZrO<sub>2</sub> phase dominating over the tetragonal phase. The sharp diffraction lines at  $2\theta = 28.3^\circ$ ,  $24.46^\circ$ , and  $31.58^\circ$  correspond to the monoclinic form and the lines at  $2\theta = 30.27^\circ$  and  $49.21^\circ$  are due to tetragonal form of ZrO<sub>2</sub>. The tetragonal phase is dominating over the monoclinic phase in the case of tungstate

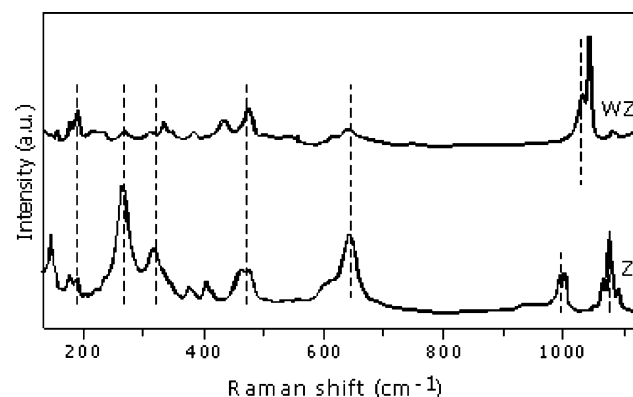


**Fig. 1** X-ray diffraction patterns of unpromoted and WO<sub>x</sub> promoted zirconia catalysts. (▼) Lines due to tetragonal phase; (Δ) Lines due to monoclinic phase

ion promoted zirconia catalyst. Further, no characteristic diffraction lines corresponding to crystalline WO<sub>3</sub> were observed, indicating a strong interaction between the dispersed WO<sub>x</sub> and the zirconia. Also there is no evidence for the formation of a new phase like Zr(WO<sub>4</sub>)<sub>2</sub>. The ammonia-TPD results (Table 1) revealed that there are at least two types of different acid sites on the WO<sub>x</sub>-ZrO<sub>2</sub> catalyst. The total amount of ammonia desorbed from the surface of W-promoted ZrO<sub>2</sub> and unpromoted ZrO<sub>2</sub> samples is observed to be 11 and 5 mL g<sup>-1</sup>, respectively.

Raman spectra of unpromoted and WO<sub>x</sub> promoted zirconia samples are shown in Fig. 2. Normally, crystalline zirconia shows characteristic Raman bands in the range 150–700 cm<sup>-1</sup> [25]. The spectrum of ZrO<sub>2</sub> exhibits Raman bands pertaining to a mixture of monoclinic (180, 188, 221, 331, 380, 476, and 637 cm<sup>-1</sup>) and tetragonal (148, 290, 311, 454, and 647 cm<sup>-1</sup>) phases and the lines due to tetragonal phase are less intense than the lines due to monoclinic phase [26, 27]. However, in the case of tungstate zirconia sample, the Raman bands due to tetragonal phase are more intense. Crystalline WO<sub>3</sub> shows characteristic Raman bands at 807, 715, and 274 cm<sup>-1</sup> [26]. Absence of these bands indicates that microcrystalline WO<sub>3</sub> is not formed on the surface of WO<sub>x</sub>-ZrO<sub>2</sub> catalyst. These results are in well-agreement with the XRD results where no independent peaks due to crystalline WO<sub>3</sub> are observed.

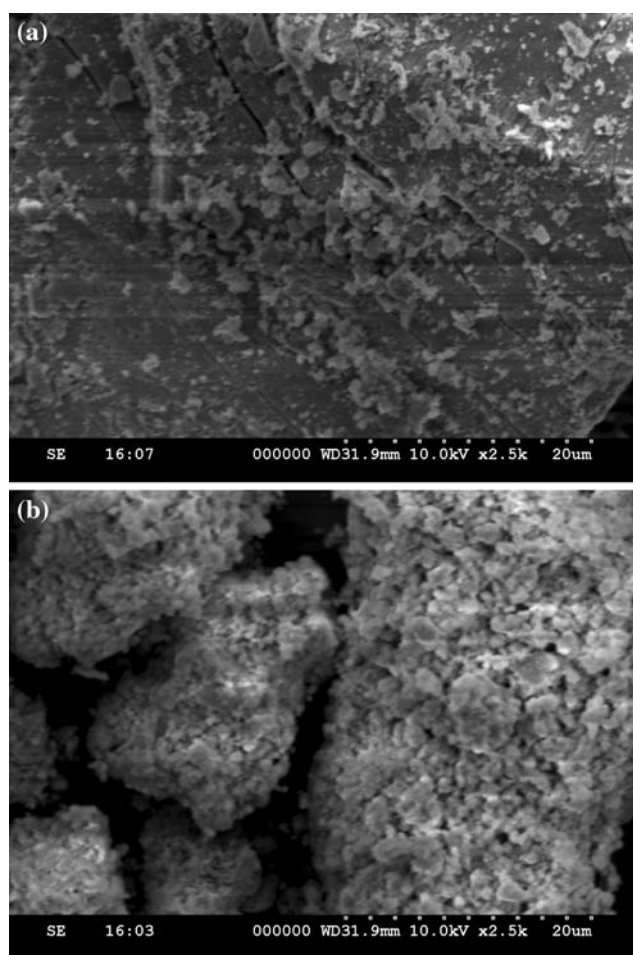
To study the surface topography and to assess the surface dispersion of WO<sub>x</sub> over the ZrO<sub>2</sub>, the SEM



**Fig. 2** Raman spectra of unpromoted and WO<sub>x</sub> promoted zirconia catalysts

**Table 1** BET surface area, total acidity, amount of monoclinic and tetragonal phases and crystallite size of ZrO<sub>2</sub> and WO<sub>x</sub>-ZrO<sub>2</sub> catalysts

Entry	Catalyst	BET SA (m <sup>2</sup> g <sup>-1</sup> )	NH <sub>3</sub> desorbed (mL g <sup>-1</sup> )	Monoclinic ZrO <sub>2</sub>		Tetragonal ZrO <sub>2</sub>	
				Amount (%)	Size (nm)	Amount (%)	Size (nm)
1	ZrO <sub>2</sub>	42	5	76	11.2	24	13.0
2	WO <sub>x</sub> -ZrO <sub>2</sub>	35	11	32	11.9	68	16.2



**Fig. 3** SEM micrographs of (a)  $\text{ZrO}_2$  and (b)  $\text{WO}_x\text{-ZrO}_2$  catalysts

investigation was performed over both zirconia and tungstated zirconia samples. The representative SEM micrographs are presented in Fig. 3. In the micrograph of zirconia, though crystallinity is observed, there are certain cracks on the surface that may be attributed to the loss of water molecules during the calcination. As can be noted from the micrograph of  $\text{WO}_x\text{-ZrO}_2$  sample, the doped  $\text{WO}_x$  is strongly interacted and highly dispersed on the surface of the zirconia support generating some porosity.

From the initial catalytic activity studies carried out with benzaldehyde (1 mmol), aniline (1 mmol), acetone (4 mmol), and catalytic amounts of  $\text{WO}_x\text{-ZrO}_2$  to fix the optimum conditions, it was observed that this reaction goes well under solvent-free conditions. Lower catalytic activities were observed when typical organic solvents, such as MeOH,  $\text{CH}_3\text{CN}$ ,  $\text{CH}_2\text{Cl}_2$ , and EtOH were employed which probably interfere with the active sites of the catalyst. Under identical conditions, the unpromoted  $\text{ZrO}_2$  catalyst exhibited insignificant product yields.

As summarized in Table 2 (Entry 1–9), the three-component reaction of different aromatic aldehydes, anilines

and cyclohexanone gave products in good to high yields (Scheme 1). In most of the cases the *syn* selectivity is more as compared to *anti* selectivity and in the case of 4-chloroaniline (Table 2, Entry 11) it is  $\sim 100\%$ . In some cases the *anti* selectivity is found to be more as compared to *syn* selectivity (Table 2, Entry 4, 7, and 9). These isomers were identified from the values of the coupling constants between the vicinal protons  $\alpha$ - and  $\beta$ - to  $\text{C}=\text{O}$ . It has been reported that the  $J$  value of *anti* isomers (ca. 7.5 Hz) is higher than those of *syn* isomers (ca. 4.5 Hz) in these types of systems (Scheme 2) [28–31]. The *anti/syn* ratio was determined by the relative areas under the absorption peaks for  $\text{H}_\beta$ . The one-pot, three-component Mannich reaction using acetophenone or acetone was also studied (Scheme 3). It was found that the corresponding  $\beta$ -amino carbonyl compounds are formed in good to moderate yields. These results are also summarized in Table 2 (Entry 10–12). Acetophenone was less reactive than the cyclohexanone and required longer reaction times to afford the desired products (Table 2, Entry 3 and 10). The spectral data for some selected representative compounds are given below:

### 3.1 2-[1-Phenyl-1-*N*-phenylamino]methylcyclohexanone (Entry 3)

IR (KBr):  $\nu = 3,451.23, 3,027, 2,924.04, 2,853.26, 1,709.61, 1,598.16, 1,570.20, 1,488.69, 1,288.39 \text{ cm}^{-1}$ .  $^1\text{H-NMR}$  (300 MHz,  $\text{CDCl}_3$ ):  $\delta = 1.73\text{--}1.81$  (m, 2H),  $1.91\text{--}1.98$  (m, 4H),  $2.36\text{--}2.38$  (m, 1H),  $2.45\text{--}2.49$  (m, 1H),  $2.73\text{--}2.77$  (m, 1H),  $4.55$  (d,  $J = 7.25 \text{ Hz}$ , 0.20 H, *anti* isomer),  $4.71$  (d,  $J = 4.35 \text{ Hz}$ , 0.80 H, *syn* isomer),  $6.47$  (d, 2H),  $6.59$  (t, 1H),  $7.01$  (t, 2H),  $7.24\text{--}7.40$  (m, 5 H) ppm. ESIMS: ( $\text{M} + 1$ )  $280 \text{ m/z}$ .

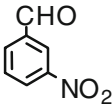
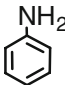
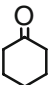
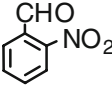
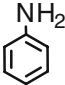
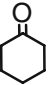
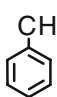
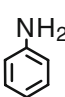
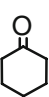
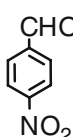
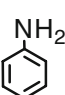

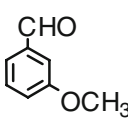
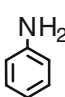
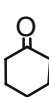
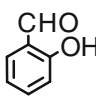
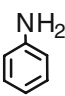
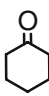
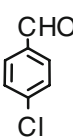
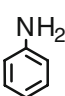
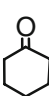
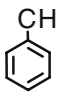
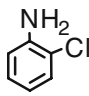
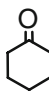
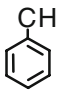
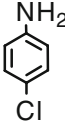
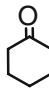
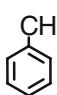
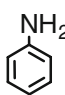
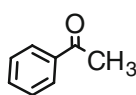
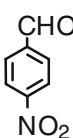
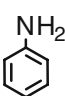
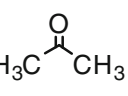
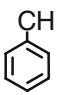
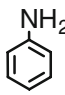
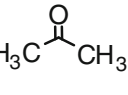
### 3.2 2-[(*p*-Nitrophenyl)(phenylamino)methyl]cyclohexanone (Entry 4)

IR (KBr):  $3,416.42, 3,045.12, 2,923, 2,853, 1,706.09$  ( $\text{C}=\text{O}$ ),  $1,598.17, 1,515.57, 1,342.92, 1,258 \text{ cm}^{-1}$ .  $^1\text{H-NMR}$  (300 MHz,  $\text{CDCl}_3$ ):  $\delta = 1.59\text{--}1.68$  (m, 1H),  $1.78\text{--}1.87$  (m, 2H),  $1.99\text{--}2.00$  (m, 1H),  $2.06\text{--}2.08$  (m, 2H),  $2.34\text{--}2.38$  (m, 1H),  $2.41\text{--}2.49$  (m, 1H),  $2.84\text{--}2.88$  (m, 1H),  $4.71$  (d,  $J = 5.85 \text{ Hz}$ , 0.60 H, *anti* isomer),  $4.83$  (d,  $J = 4.39 \text{ Hz}$ , 0.40 H, *syn* isomer),  $6.48$  (d, 2H),  $6.67$  (d, 1H),  $7.07$  (t, 2H),  $7.58$  (t, 2H),  $8.17$  (d, 2H) ppm. ESIMS: ( $\text{M} + 1$ )  $325 \text{ m/z}$ .

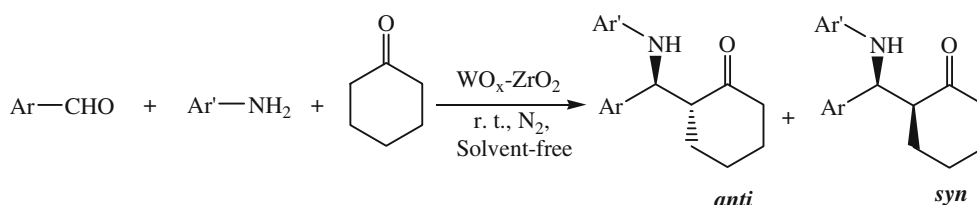
### 3.3 2-[1-(*p*-Chlorophenyl)-1-*N*-phenylamino]methylcyclohexanone (Entry 7)

IR (KBr):  $\nu = 3,385.77, 3,020.71, 2,924.28, 2,854.39, 1,706.06, 1,600.50, 1,493.44, 1,457.29, 1,313.74, 752.04 \text{ cm}^{-1}$ .  $^1\text{H-NMR}$  (500 MHz,  $\text{CDCl}_3$ ):  $\delta = 1.74\text{--}1.80$

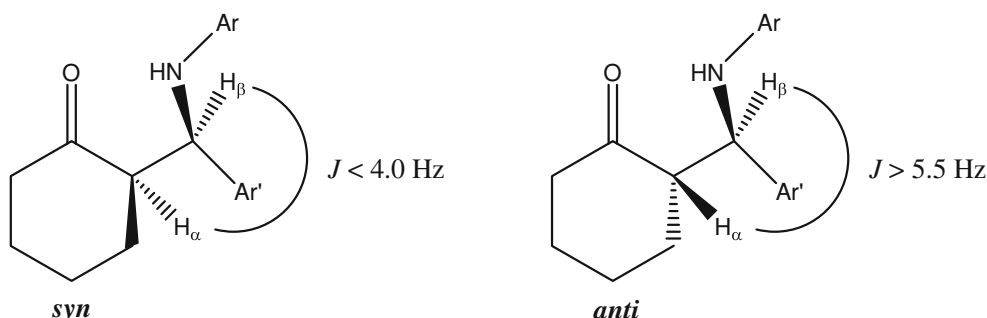
**Table 2** Direct Mannich-type reactions of aromatic aldehydes, anilines, and ketones employing  $\text{WO}_x\text{-ZrO}_2$  catalyst at ambient temperature and solvent-free conditions

Entry	Aldehyde	Amine	Ketone	Time (min)	Yield (%)	<i>anti:syn</i>
1.				75	82	30:70
2.				240	86	26:74
3.				135	90	20:80
4.				60	89	60:40
5.				100	86	25:75
6.				90	78	30:70
7.				120	84	70:30
8.				120	66	74:26
9.				180	82	~ 00:100
10.				480	80	—
11.				210	92	—
12.				180	79	—



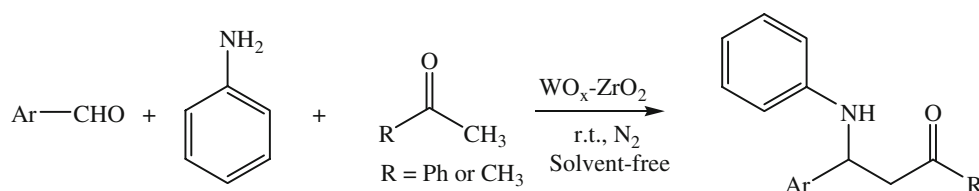


**Scheme 1** Three-component reaction of aromatic aldehyde, aniline, and cyclohexanone catalyzed by tungstated zirconia



**Scheme 2** The  $J$  values of *syn* and *anti* isomers

**Scheme 3** Three-component reaction of aromatic aldehyde, aniline, and acetone/acetophenone catalyzed by tungstated zirconia



(m, 3 H), 1.95–2.01 (m, 3 H), 2.34–2.37 (m, 1 H), 2.43–2.47 (m, 1 H), 2.74–2.75 (m, 1 H), 4.538 (d,  $J = 6.043$  Hz, 0.70 H, *anti* isomer), 4.654 (d,  $J = 3.778$  Hz, 0.30 H, *syn* isomer), 6.433 (d, 2H), 6.658 (t, 1H), 7.01 (t, 2 H), 7.19–7.35 (m, 4H) ppm. ESIMS: ( $M + 1$ ) 314  $m/z$ .

## 4 Conclusions

An efficient  $\text{WO}_x\text{-ZrO}_2$  solid acid catalyst was synthesized from zirconium hydroxide gel obtained by a coprecipitation method, and impregnating with ammonium metatungstate. The physicochemical characterization was carried out using various techniques including Raman spectroscopy and ammonia-TPD. The XRD results revealed that tetragonal phase dominates over the monoclinic phase in the case of tungstated zirconia catalyst. Further, no XRD lines corresponding to crystalline  $\text{WO}_3$  were observed, indicating a strong interaction and high dispersion of  $\text{WO}_x$  over the zirconia. The ammonia-TPD results suggested that there are at least two types of different acid sites on the tungstated zirconia. The synthesized catalyst was found to efficiently catalyze the three-

component Mannich-type reaction under solvent-free conditions at ambient temperature. Mild reaction temperature, solvent-free conditions, high yield of the products and short reaction times are some of the advantages associated with this protocol.

**Acknowledgments** MKP thanks the Council of Scientific and Industrial Research (CSIR), New Delhi, India for a Senior Research Fellowship. BTR thanks the Department of Science and Technology, New Delhi, India for a Junior Research Fellowship in the SERC scheme (SP/S1/PC-31/2004).

## References

1. Clark JH (2002) *Acc Chem Res* 35:791–797
2. Corma A (1995) *Chem Rev* 95:559–614
3. Corma A, Garcia H (2003) *Chem Rev* 103:4307–4365
4. Okuhara T (2002) *Chem Rev* 102:3641–3665
5. Hamer MA, Sun Q (2001) *Appl Catal A: Gen* 221:45–62
6. Olah GA, Prakash GKS, Sommer J (1985) *Superacids*. Wiley, New York
7. Olah GA, Takashi K, David M (1978) *Synthesis* 929–938
8. Guttman AT, Grasselli RK (1983) *Appl Catal* 9:57–67
9. Dupont P, Vedrine JC, Paumard E, Hecquet G, Lefebvre F (1995) *Appl Catal A: Gen* 129:217–227

10. Arata K, Matsushashi H, Hino M, Nakamura H (2003) *Catal Today* 81:17–30
11. Gillespie RJ, Peel TE (1973) *J Am Chem Soc* 95:5173–5179
12. Yadav GD, Nair JJ (1999) *Microporous Mesoporous Mater* 33:1–48
13. Reddy BM, Sreekanth PM, Reddy VR (2005) *J Mol Catal A: Chem* 225:71–78
14. Reddy BM, Sreekanth PM, Lakshmanan P (2005) *Mol Catal A: Chem* 237:93–100
15. Reddy BM, Patil MK, Rao KN, Reddy GK (2006) *J Mol Catal A: Chem* 258:302–307
16. Reddy BM, Patil MK (2008) *Curr Org Chem* 12:118–140
17. Hino M, Arata K (1988) *J Chem Soc Chem Commun* 1259–1260
18. Arata K, Hino M (1989) *Chem Lett* 971–972
19. Reddy BM, Sreekanth PM (2002) *Syn Commun* 32:2815–2819
20. Sarish S, Devassy BM, Bohringer W, Fletcher J, Halligudi SB (2005) *J Mol Catal A: Chem* 240:123–131
21. Reddy BM, Reddy VR, Giridhar D (2001) *Syn Commun* 31:3603–3607
22. Arend M, Westermann B, Risch N (1998) *Angew Chem Int Ed* 37:1044–1070
23. Tramontini M, Angiolini L (1994) *Mannich-bases: chemistry and uses*. CRC Press, Boca Raton, Florida
24. Volkmann RA (1991) In: Trost BM, Fleming I (eds) *Comprehensive organic synthesis*, vol 1. Pergamon Press, Oxford, pp 355–396
25. Kuba S, Heydorn PC, Grasselli RK, Gates BC, Che M, Knözinger H (2001) *Phys Chem Chem Phys* 3:146–154
26. Scheithauer M, Jentoft RE, Gates BC, Knözinger H (2000) *J Catal* 191:271–274
27. Scheithauer M, Grasselli RK, Knözinger H (1998) *Langmuir* 14:3019–3029
28. Loh TP, Liung SBKW, Tan K-L, Wei L-L (2000) *Tetrahedron* 56:3227–3237
29. Gennari C, Venturini I, Gislón F, Schimperma G (1987) *Tetrahedron Lett* 28:227–230
30. Guanti G, Narisano E, Banfi L (1987) *Tetrahedron Lett* 28:4331–4334
31. Ollevier T, Nadeau EJ (1994) *J Org Chem* 69:9292–9295